

GA-A24846

**SEARCH FOR A CRITICAL
ELECTRON TEMPERATURE GRADIENT
IN DIII-D L-MODE DISCHARGES**

by

J.C. DeBOO, S. CIRANT, T.C. LUCE, A. MANINI, C.C. PETTY, F. RYTER,
M.E. AUSTIN, D.R. BAKER, K. GENTLE, C.M. GREENFIELD,
J.E. KINSEY, and G.M. STAEBLER

SEPTEMBER 2004

DISCLAIMER

This report was prepared as an account of work sponsored by an agency of the United States Government. Neither the United States Government nor any agency thereof, nor any of their employees, makes any warranty, express or implied, or assumes any legal liability or responsibility for the accuracy, completeness, or usefulness of any information, apparatus, product, or process disclosed, or represents that its use would not infringe privately owned rights. Reference herein to any specific commercial product, process, or service by trade name, trademark, manufacturer, or otherwise, does not necessarily constitute or imply its endorsement, recommendation, or favoring by the United States Government or any agency thereof. The views and opinions of authors expressed herein do not necessarily state or reflect those of the United States Government or any agency thereof.

SEARCH FOR A CRITICAL ELECTRON TEMPERATURE GRADIENT IN DIII-D L-MODE DISCHARGES

by

J.C. DeBOO, S. CIRANT,^{*} T.C. LUCE, A. MANINI,[†] C.C. PETTY, F. RYTER,[†]
M.E. AUSTIN,[‡] D.R. BAKER, K. GENTLE,[‡] C.M. GREENFIELD,
J.E. KINSEY,[^] and G.M. STAEBLER

This is a preprint of a paper to be presented at the 20th IAEA
Fusion Energy Conference, Vilamoura, Portugal, November 1-6,
2004 and to be published in the *Proceedings*.

^{*}Instituto di Fisica del Plasma, CNR, Milano, Italy.

[†]Institut fur Plasmaphysik, Garching, Germany.

[‡]University of Texas at Austin, Austin, Texas.

[^]Lehigh University, Bethlehem, Pennsylvania.

Work supported by
the U.S. Department of Energy
under DE-FC02-04ER554698,
DE-FG03-97ER54415, and DE-FG02-92ER54141

GENERAL ATOMICS PROJECT 30200
SEPTEMBER 2004

Search for a Critical Electron Temperature Gradient in DIII-D L-Mode Discharges

J.C. DeBoo 1), S. Cirant 2), T.C. Luce 1), A. Manini 3), C.C. Petty 1), F. Rytter 3),
M.E. Austin 4), D.R. Baker 1), K.W. Gentle 4), C.M. Greenfield 1),
J.E. Kinsey 5), and G.M. Staebler 1)

- 1) General Atomics, P.O. Box 85608, San Diego, California 92186-5608, USA
- 2) Instituto di Fisica del Plasma, CNR, Milano, Italy
- 3) IPP-Garching, Garching, Germany
- 4) University of Texas at Austin, Austin, Texas, USA
- 5) Lehigh University, Lehigh, Pennsylvania, USA

e-mail contact of main author: deboo@fusion.gat.com

Abstract. Two experiments on DIII-D have been performed with the purpose of searching for evidence of a critical electron temperature gradient or gradient scale length. Both experiments employed off-axis EC heating to vary the local value of $\nabla T_e/T_e$ while holding the total heating power and thus edge temperatures constant. No evidence of an inverse critical gradient scale length, k_{crit} , was observed in these experiments, but the existence of one cannot be ruled out by the experimental results. If k_{crit} exists, the experimental results indicate $k_{\text{crit}} < 3.8 \text{ m}^{-1}$ at $\rho = 0.45$ and $k_{\text{crit}} < 2.5 \text{ m}^{-1}$ at $\rho = 0.29$ corresponding to a critical gradient scale length larger than 43% and 65% of the plasma minor radius, respectively. Models other than one based on k_{crit} are also consistent with the experimental observations.

1. Introduction

Electron transport in experiments on some tokamaks, notably ASDEX Upgrade [1], has been successfully modeled with a model of the form

$$\chi_e = \chi_o + f(T_e)[(\nabla T_e/T_e) - k_{\text{crit}}]H_k \quad (1)$$

where χ_o can be a function of T_e but is independent of ∇T_e and is small compared to the critical gradient term. The model shows that the incremental or heat pulse diffusivity,

$$\chi_e^{\text{HP}} \equiv \partial(\chi_e \nabla T_e) / \partial \nabla T_e = \chi_o + f(T_e)[2(\nabla T_e/T_e) - k_{\text{crit}}]H_k \quad (2)$$

undergoes a discontinuous increase when the local inverse temperature gradient scale length, $1/L_{T_e} = \nabla T_e/T_e$, exceeds a critical value, k_{crit} , and the Heaviside function, H_k , becomes nonzero. This jump in χ_e^{HP} produces a nonlinear change in T_e as k_{crit} is exceeded.

Two different experiments in DIII-D, one using a novel technique to modulate the local electron temperature gradient and the other designed to perform a systematic variation of local electron heat flux, were performed to search for evidence of the existence of k_{crit} . Results from these experiments show no evidence of a nonlinear response in T_e nor any evidence of a critical gradient scale length. However, the results cannot rule out the possible existence of k_{crit} . The experimental results on DIII-D reported here are similar to those reported for ASDEX Upgrade [1] and indicate that if a critical gradient scale length exists in the plasmas studied then the observations were all made at values above k_{crit} , i.e., $\nabla T_e/T_e|_{\text{exp}} > k_{\text{crit}}$. These results are consistent with previous experiments on DIII-D [2] where modulated ECH used to probe the T_e profile showed no evidence of nonlinear behavior.

2. ECH Swing Experiments

The ECH swing experiments in DIII-D were designed to search for evidence of the existence of k_{crit} utilizing a novel technique first employed on FTU [3]. The technique utilizes two different electron cyclotron heat pulse trains, ECH1 and ECH2, each absorbed at slightly different radii and modulated out of phase with respect to each other in order to localize the change in ∇T_e at a constant total input power. This keeps the overall T_e profile roughly constant outside the probed region while locally changing ∇T_e . In the deposition region where ECH1 and ECH2 overlap, the EC power is constant and thus no modulation in T_e is expected if the two heat pulses simply linearly combine. However if nonlinear changes in χ^{HP} occur they will modulate T_e and produce a non-zero amplitude in the Fourier analyzed T_e response.

The experiments were carried out in sawtooth-free, deuterium, L-mode discharges, limited on the inside wall of the vessel to prevent transitions to H-mode with $I_p = 0.8$ MA, $B_T = 2.0$ T and with $P_{\text{ECH1}} \sim P_{\text{ECH2}} \sim 1$ MW square wave modulated at 25 Hz with a 50% duty cycle. The temperature gradient was probed at two spatial locations, $\rho = 0.2-0.3$ and $0.4-0.5$, and at the inner location three heat flux conditions were tested with 0, 2.8 and 4.0 MW NBI. The line average density varied from $1.5 \times 10^{19} \text{ m}^{-3}$ in the Ohmic discharges to $2.9 \times 10^{19} \text{ m}^{-3}$ with 4 MW of NBI. The electron temperature and density profiles for the Ohmic condition are shown in Fig. 1 where it is also shown that the ratio of T_i/T_e becomes less than one for $\rho \leq 0.65$, a condition favorable for stabilization of electron temperature gradient (ETG) drift waves. Thus, ETG modes are not expected to contribute to transport in the plasma regions studied. The temperature and density gradients in the regions of interest favor destabilization of trapped electron modes (Sec. 4).

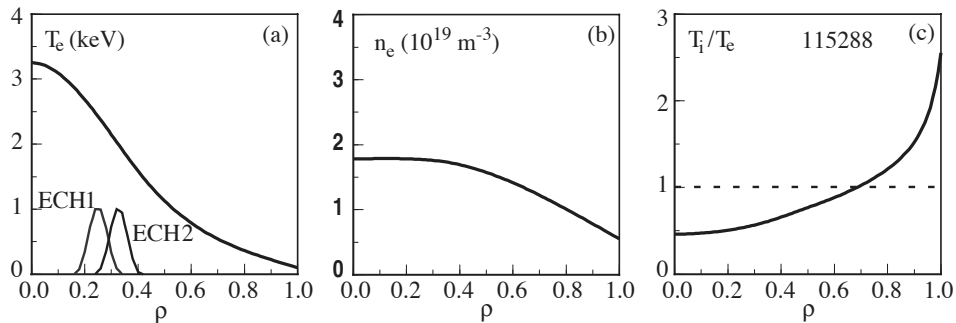


Fig. 1. Profiles of (a) electron temperature and ECH deposition, (b) electron density and (c) ratio of ion to electron temperature for an L-mode discharge without NBI and plasma current 0.8 MA.

The maximum change in ∇T_e was produced in the Ohmic condition with ECH resonant at $\rho = 0.2-0.3$. The change in $-\nabla T_e/T_e$ as a function of time is displayed in Fig. 2 along with the T_e profile between the two ECH deposition regions at times near the end of each of the periods with ECH1 and ECH2 on. The alternate application of power at ECH1 and ECH2 produces a modulation in the temperature gradient at nearly constant T_e at $\rho = 0.27$. The gradient is determined by differencing adjacent channels of the electron cyclotron emission system [4] after first phase-lock averaging over nine modulation periods. It is clear that when ECH2 is on, the inverse scale length decreases in the spatial region between the two deposition regions while it increases with ECH1 on. The maximum variation in $-\nabla T_e/T_e$ observed was from 2.3 to 6.7 m^{-1} . The relative change in ∇T_e was over 100% in the Ohmic case with smaller changes produced in the cases with NBI power and at larger ρ , making these cases less likely to exceed a critical value.

No evidence of a nonlinear response in T_e was observed in the Ohmic condition where it was expected that such a response was most likely to occur nor in any of the other conditions studied, consistent with earlier experiments [2]. To search for an indication of a nonlinear T_e response, three discharges were taken at each condition, one with ECH1 and ECH2 modulated out of phase [Case 1+2, Fig. 3(c)] and then one each with ECH1 modulated and ECH2 CW at half power (Case 1) and vice versa (Case 2). Cases 1 and 2 are executed with the CW source at half power in order to keep the total average power fixed, making the plasma profiles very similar in all three cases. The detailed search for evidence of nonlinear behavior was carried out by comparing the Fourier analyzed amplitude and phase of the T_e modulations from Case 1+2 to a calculation of the linear combination of Fourier amplitudes and phases from Case 1 and Case 2 (Fig. 3). In the overlap region between ECH1 and ECH2 there is little or no power modulation since the two sources are modulated 180 deg. out of phase with respect to each other even though the temperature gradient is dramatically changing in this region. Thus one expects a simple linear combination of pulse amplitudes of ECH1 and ECH2 to become small in this region and phases to jump by 180 deg. on either side of the point where the amplitude is minimum. If however the variation in ∇T_e produces a nonlinear variation in χ^{HP} , then a nonlinear variation in T_e may be produced. Thus, the clearest evidence for nonlinear behavior would be an amplitude in Case 1+2 considerably different than the simple linear combination of Case 1 and Case 2 in the overlap region. The amplitude could be larger or smaller than the linear combination depending on the phase of the nonlinear response. However, as shown in Fig. 3 the amplitude and phase in Case 1+2 is the same as the linear combination, indicating no nonlinear behavior in χ^{HP} is required to understand the T_e

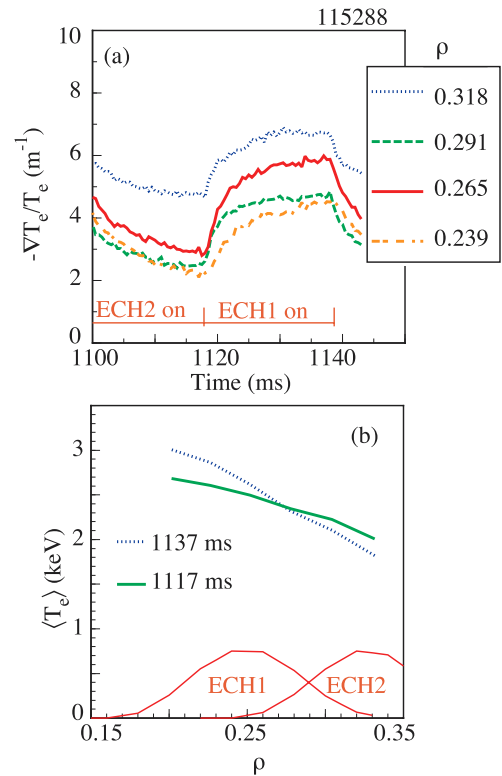


Fig. 2. (a) Variation of inverse temperature gradient scale length with time for four ECE channels in the ECH deposition region. (b) Temperature profile in the ECH deposition region near the end of ECH1 and ECH2 phase-lock averaged over nine modulation periods, 360 ms.

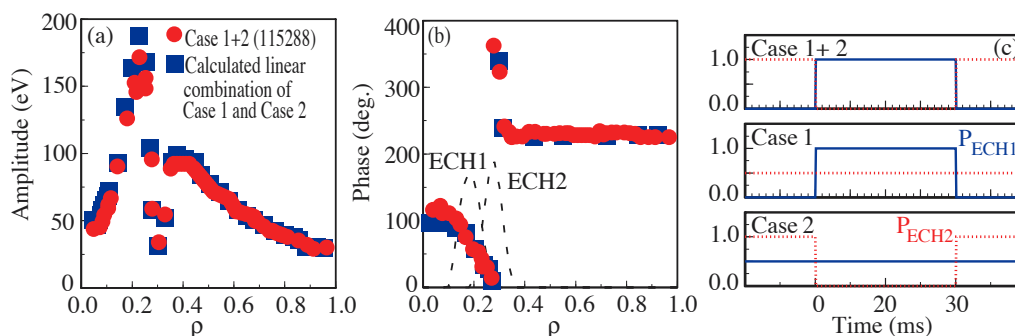


Fig. 3. (a) Fourier amplitude and (b) phase components of the electron temperature response at the fundamental frequency for the Ohmic condition with ECH1 and ECH2 applied out of phase with respect to each other (circles) and applied individually and then linearly combined (squares). (c) Power modulation for the three cases.

response to the applied heat pulses. In an attempt to provide additional power to help excite a nonlinear resonance, CW power from an additional gyrotron was applied at $r = 0.3$ but again no evidence of a nonlinear response was observed.

Modeling of the measured pulse propagation characteristics indicates that a step in χ^{HP} is consistent with the pulse amplitude in Case 2 but two steps are required to obtain agreement with the pulse amplitude in Case 1 and the phase is not well matched in either case. The same model cannot explain Case 1+2, specifically designed to look for nonlinear behavior.

3. Electron Heat Flux Scan Experiments

The DIII-D experiments described here closely followed experiments first done on ASDEX Upgrade [1] where the inverse electron temperature gradient scale length $\nabla T_e/T_e$ was varied shot-by-shot by varying the electron heat flux while holding the heat flux at the plasma edge and thus the total power constant. This approach results in the edge temperature remaining fixed while allowing a local variation in heat flux. A systematic variation in heat flux was accomplished by applying ECH at two locations in the plasma confinement region, ECH1 and ECH2, near the half radius and varying the power at each location on a shot by shot basis while holding the sum of the powers constant. This experiment in DIII-D and the ECH swing experiment were similar in that both kept the total power and temperatures at larger radii, beyond the ECH deposition region, constant. They differ in that the heat flux scan and $\nabla T_e/T_e$ variation was accomplished shot by shot, primarily with CW ECH, while the ECH swing experiment varied $\nabla T_e/T_e$ during each shot with modulated ECH. The separation between ECH1 and ECH2 was much larger in the heat flux scan experiments.

The target plasmas used in the DIII-D heat flux scan experiments were very similar to those employed in the ECH swing experiments described above with no NBI heating except early in the discharge to delay the onset of sawteeth and with $n_e = 1.7 \times 10^{19} \text{ m}^{-3}$. The experiments were performed during the sawtooth-free portion of the discharges. The plasma parameters were also very similar to those in [1] and thus allow a direct comparison of results between the two tokamaks. Four gyrotron tubes with approximately 0.5 MW per gyrotron at 110 GHz were used to systematically vary the power resonant at ECH1 and ECH2. Since the toroidal field and thus the safety factor $q_a \sim 7$ were held constant, the deposition location for each gyrotron was changed shot by shot by moving a poloidal steering mirror in the ECH launchers. The range in T_e profiles produced in this manner is shown in Fig. 4. The profiles outside ECH2 are very similar as expected since the surface integrated heat flux (Fig. 5) is

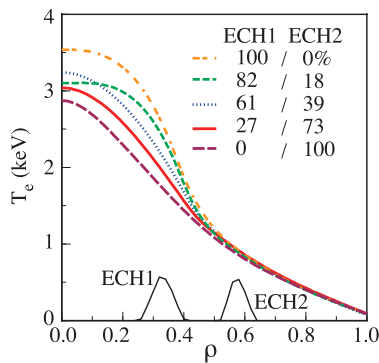


Fig. 4. Electron temperature profiles produced by varying the amount of EC power resonant at ECH1 and ECH2. The percentage of total EC power at each location is displayed in the figure for each profile. Plasma parameters were $I_p = 0.8$ MA, line averaged density $1.7 \times 10^{19} \text{ m}^{-3}$, $B_T = 2.0$ T and $q_a = 7$.

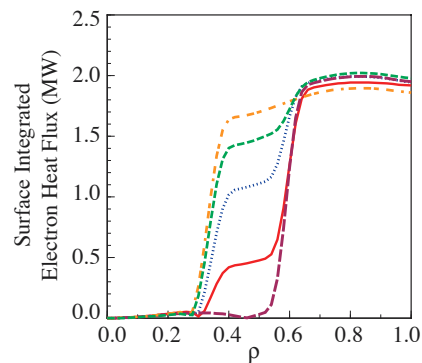


Fig. 5. Surface integrated electron heat flux vs. normalized plasma radius for the same conditions and line types in Fig. 4. Ohmic heating is responsible for the heat flux in the plasma core.

constant in this region for all discharges. One advantage of performing the experiments with this technique is that the local value of ∇T_e can be varied while producing very little change in the local T_e between ECH1 and ECH2 as compared to performing a neutral beam power scan for instance where the entire T_e profile would change. Thus, $\nabla T_e/T_e$ was varied at essentially constant T_e allowing just the ∇T_e dependent term in Eqns. (1) and (2) to be probed. The surface integrated electron heat flux shown in Fig. 5 is due to ECH and Ohmic heating. Power balance analysis was performed using the ONETWO transport code [5]. The total power in the electrons is ~ 2 MW with about 0.5 MW due to Ohmic heating. Conduction is the dominant power loss overall and at the location of interest between ECH1 and ECH2, $\rho = 0.45$ where the heat flux was systematically varied from shot to shot, the loss due to radiation and collisional transfer of energy to the ions is small, about 0.1 MW each. Convection is negligible in these discharges.

In order to obtain information about χ^{HP} which characterizes the dynamic thermal response of the electrons, the power on one of the gyrotrons was modulated. Typically a gyrotron at ECH2 was modulated at 28 Hz with a square wave pulse at a 50% duty cycle. The electron temperature response measured by the electron cyclotron emission system was Fourier analyzed and the spatial derivative of the resulting pulse amplitude and phase based on slab geometry was used to estimate χ^{HP} [6]. The response at the third harmonic was used in the analysis in order to diminish the impact of the frequency dependence of the transport coefficients and to reduce the potential impact of any transport terms due to convection.

No evidence of a critical gradient scale length was observed in these experiments but the existence of one cannot be ruled out. The normalized diffusivity for both the power balance analysis and heat pulse analysis is displayed in Fig. 6 as a function of $\nabla T_e/T_e$. The diffusivity is normalized by $T_e^{3/2}$ to take out the effect of the small changes in T_e at $\rho = 0.45$ (Fig. 4) based on a gyro-Bohm-like temperature dependence. The trend in $\chi^{HP}/T_e^{3/2}$ clearly decreases as $\nabla T_e/T_e$ decreases, but there is no evidence of a discontinuous drop in diffusivity at some critical value of $\nabla T_e/T_e$ as suggested by k_{crit} in Eq. (2). The results of this experiment are consistent with the results from ASDEX Upgrade [1] as the values and trends agree very well with each other (Fig. 6). There are three DIII-D points in Fig. 6 however, that display a similar trend but at heat pulse diffusivity values much larger than the other points. The key parameters responsible for this are as yet unidentified but the global plasma parameters and the power balance diffusivity for these points are similar to the other discharges. The trend in the power balance diffusivity is also interesting in that it clearly does not extrapolate back to the origin of the graph, indicating that there is not a simple linear relation between power balance diffusivity and $\nabla T_e/T_e$. It is possible that a critical inverse gradient scale length exists but it must be at values $k_{crit} < 3.8 \text{ m}^{-1}$, the lowest value achieved in these experiments. This value corresponds to a scale length $L_{Te} > 0.26 \text{ m}$ or 43% of the plasma minor radius. This is a relatively large temperature scale length that is normally found only close to the center of L-mode plasmas in DIII-D, typically $\rho \leq 0.3$. So if k_{crit} exists, it is exceeded in typical L-mode temperature profiles over most of the plasma minor radius. Observation of any T_e

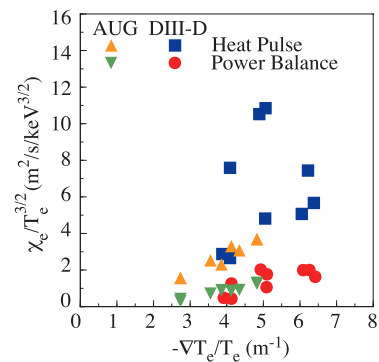


Fig. 6. Normalized thermal diffusivity at $\rho = 0.45$ vs. the inverse temperature gradient scale length based on heat pulse propagation (squares, upright triangles) and power balance (circles, inverted triangles) analysis. Experimental results from ASDEX-Upgrade (triangles) are discussed in [1] and are at similar plasma current, density and safety factor as in DIII-D.

profiles going from below to above k_{crit} would be limited to the very center of typical L-mode discharges in DIII-D where often sawteeth provide the major thermal transport mechanism.

4. Discussion

Additional estimates of an upper bound on k_{crit} can be obtained from the ECH swing experiments. At $\rho = 0.29$, where the heat pulses from ECH1 and ECH2 nearly completely cancel each other, values of $\nabla T_e/T_e$ varied from 2.5 to 5 m^{-1} (Fig. 2) without any evidence of nonlinear behavior. It is clear that the temperature profile response is not very stiff since $\nabla T_e/T_e$ was increased at least a factor of 2 above k_{crit} , if k_{crit} exists. At $\rho = 0.24$ somewhat lower values of $\nabla T_e/T_e$ were obtained but in this region it is not as clear as to whether one would expect to observe nonlinear behavior since at this location effects from the heat pulse at ECH1 are expected to dominate and potentially mask any nonlinear response. Also for the ASDEX Upgrade data in Fig. 6 a fit of the heat pulse and power balance data to Eqn. (1) and (2) resulted in an estimate of $k_{\text{crit}} = 2.3 \text{ m}^{-1}$ at $\rho = 0.5$ [1] which is just below the lowest $\nabla T_e/T_e$ values shown in Fig. 6 for ASDEX Upgrade.

Based on analysis with a linear gyrokinetic stability code with noncircular plasma geometry, GKS [7], trapped electron modes (TEMs) dominate the drift wave spectrum of instabilities in the spatial region of interest for the heat flux scan experiments and the low density ECH swing experiments discussed above. The calculations indicate that TEMs are the most unstable modes with the largest growth rates in the region analyzed, $0.2 < \rho < 0.7$, and have wavenumbers at the maximum growth rates in the range $k=1.4\text{--}6 \text{ cm}^{-1}$. Generally, k at the maximum growth rate increases with minor radius in this region. The spectral range of wavenumbers at $\rho = 0.44$ is displayed in Fig. 7 which indicates a spectral width of $\sim 2 \text{ cm}^{-1}$. The experimental observations indicate that if a critical gradient exists it is likely to exist near the plasma core where lower values of $\nabla T_e/T_e$ exist. The GKS calculations indicate that the threshold for TEMs is at $\rho \leq 0.2$, consistent with k_{crit} near the plasma core if TEMs are responsible for k_{crit} .

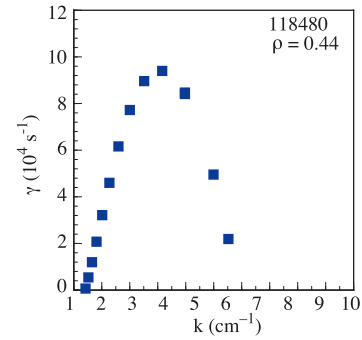


Fig. 7. Growth rate for trapped electron modes vs. wavenumber at normalized plasma radius of $\rho=0.44$ based on linear gyrokinetic stability calculations with the GKS code.

Although the DIII-D experimental results are consistent with a model for thermal diffusivity based on a critical temperature gradient scale length, the results do not compel one to employ only this type of model. Two other possible dependencies of $\chi^{\text{HP}}/T_e^{3/2}$ on $\nabla T_e/T_e$ are shown in Fig. 8 along with a critical gradient dependence shown in Fig. 8(c) based on Eq. (2). The offset linear dependence in Fig. 8(a) leads to negative values of χ^{HP} for $\nabla T_e/T_e < 2 \text{ m}^{-1}$ which implies that local heat flux decreases as the temperature gradient becomes steeper, perhaps due to a heat pinch. A nonlinear dependence such as $(-\nabla T_e/T_e)^\alpha$ is displayed in Fig. 8(b). Based on previous experiments α cannot be too large or a stiff profile response would result which was not observed [2]. A fit of the data yields $\alpha \sim 5/3$ for low values of χ^{HP} at $\nabla T_e/T_e = 0$. For the critical gradient dependent model k_{crit} was arbitrarily chosen at 3 m^{-1} just to illustrate the general dependence of the model. It should be noted however that the smaller k_{crit} becomes, the smaller the jump in χ^{HP} becomes until the jump becomes negligibly small near $k_{\text{crit}} = 2 \text{ m}^{-1}$. This may be why if a critical temperature gradient scale length exists, evidence for a jump in χ^{HP} associated with it has proven difficult to observe experimentally.

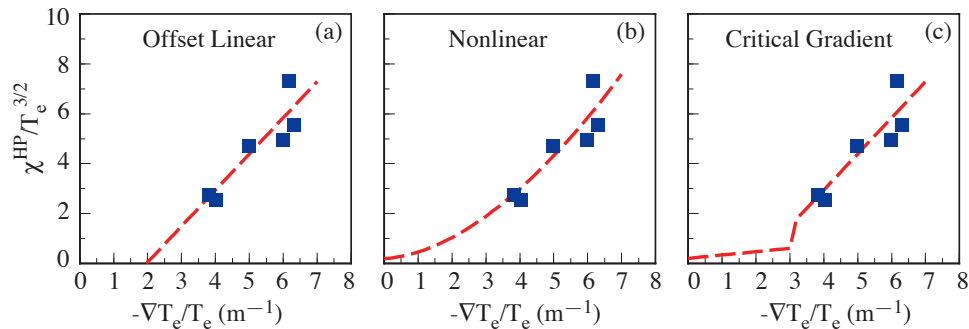


Fig. 8. Dependences of normalized heat pulse diffusivity on inverse temperature gradient scale length allowed by the experimental results include (a) an offset linear dependence, (b) a nonlinear dependence and (c) a critical gradient dependence as expressed in Eq. (2).

5. Summary and Conclusions

Two experiments on DIII-D have been performed with the purpose of searching for evidence of a critical electron temperature gradient or gradient scale length where the dynamic electron transport or heat pulse transport changes dramatically in going from below to above a critical or threshold value. Both experiments employed off-axis EC heating to vary the local value of $\nabla T_e/T_e=1/L_{Te}$ while holding the total heating power and thus edge temperature constant. The ECH swing experiment varied $1/L_{Te}$ in a time dependent manner using modulated ECH during individual discharges at two spatial locations, $\rho = 0.2-0.3$ and $\rho = 0.4-0.5$, and three heat flux conditions. The second experiment varied $1/L_{Te}$ with application of CW ECH, varying the local heat flux at $\rho = 0.45$ from discharge to discharge, again at constant edge temperatures. No evidence of a critical gradient scale length, k_{crit} , was observed in these experiments, but the existence of one cannot be ruled out by the experimental results. If k_{crit} exists, the experimental results indicate $k_{crit} < 3.8 m^{-1}$ at $\rho = 0.45$ and $k_{crit} < 2.5 m^{-1}$ at $\rho = 0.29$ corresponding to a critical gradient scale length larger than 43% and 65% of the plasma minor radius, respectively. Models other than one based on k_{crit} are also consistent with the experimental observations such as an offset linear or power law dependence of χ_{HP} on $1/L_{Te}$.

Acknowledgment

This work was supported by the U.S. Department of Energy under DE-FC02-04ER54698, DE-FG03-97ER54415, and DE-FG02-92ER54141.

References

- [1] RYTER, F., *et al.*, Nucl. Fusion **43** (2003) 1396.
- [2] DEBOO, J.C., *et al.*, in Proc. of 29th European Physical Society Conference on Plasma Physics and Controlled Fusion, Montreux, Switzerland, 2002.
- [3] CIRANT, S., *et al.*, Plasma Phys. Control. Fusion Research (Proc. of 19th IAEA Conf., Lyon, France, 2002) IAEA-CN-94/EX/C4-2Rb.
- [4] AUSTIN, M.E., and LOHR, J., Rev. Sci. Instrum. **74** (2003) 1457.
- [5] ST JOHN, H.E., *et al.*, Plasma Phys. Control. Fusion Research (Proc. of 15th IAEA Conf., Seville, Spain, 1994), Vol. 3 (1995) p. 603.
- [6] LOPES CARDOZO, N.J., Plasma Phys. Control. Fusion **37** (1995) 799.
- [7] WALTZ, R.E., and MILLER, R.L., Phy. Plasmas **6** (1999) 4265.